ALKIMIA : Jurnal Ilmu Kimia dan Terapan

ARTICLES

View Article Online
View Journal | View Issue

OPEN ACCESS

Synthesis of Fe_3O_4 Nanocatalyst Capped Citric Acid (Fe_3O_4-CA) from *Sargassum filipendula*

Dian Pratiwi[a]*

Abstract. The nanocatalyst Fe_3O_4 capped citric acid (Fe_3O_4-CA) was successfully synthesized using brown seaweed Sargassum filipendula. Sulfated polysaccharides in Sargassum filipendula extract contain sulfate, hydroxyl, and aldehyde groups which cause Fe^{3+} reduction and nanoparticle stabilization. The FT-IR results of Sargassum filipendula extract showed the presence of C-O-SO_3 stretching vibrations at 1040 cm^{-1}, sulfate groups at 1241 cm^{-1}, aromatic C-C at 1413 cm^{-1}, carbonyl at 1604 cm^{-1}, C-H stretching vibrations at 2932 cm^{-1}, and the hydroxyl group at 3316 cm-1. Meanwhile, citric acid was used as capping to prevent agglomeration of the synthesized nanocatalyst. Fe_3O_4-CA nanocatalyst were characterized using XRD, PSA, and SEM-EDX. The XRD results were processed using the Debye-Scherrer equation and the crystal size of Fe_3O_4-CA was 8.5 nm. PSA results show that Fe_3O_4-CA particles has an average radius of 45.09 nm. This nanocatalyst was also tested for the synthesis of pyrimidine-derivative compound at optimum conditions using 7.5% mol of Fe_3O_4-CA catalyst, 50 °C for 6 hours, in order to obtain a yield of 83.2%.

Keywords : Fe_3O_4, Nanocatalyst, *Sargassum filipendula*

[a]*Poltekkes Kemenkes Medan, Jalan Jamin Ginting KM 13.5, Medan 20137, Indonesia*
Correspondence and requests for materials should be addressed to Pratiwi, D.
(email: dianpratiwitlm@gmail.com)

Introduction

Nanocatalyst have a size of 1-100 nm. Reducing the dimensions of the catalyst to nano size will certainly increase the surface area of the catalyst and consequently increase the activity of the catalyst in certain reactions. The fineness and size of the nanocatalyst formed is influenced by at least 3 factors, namely the heating temperature in the nanocatalyst manufacturing process, continuous media, and the time used [1]. These three things need to be controlled and varied in the process of making nanocatalyst. The higher the temperature used in the nanocatalyst manufacturing process, the better the interaction of the nanocatalyst base material with the continuous media used [2]. However, as the reaction temperature increases, this means that more energy is needed and equipment that is more capable of withstanding higher heat will result in higher costs [3].

Nanocatalyst of varied shapes and sizes can be synthesized by using physical, chemical, or biological pathways. However, exploiting physical and chemical routes lead to high energy consumption, low yield, high cost, and environmental damage by employing harsh reducing agents. The biological pathways involve the use of microorganisms (bacteria, fungi, yeast, algae, etc.) or plants, and using microorganisms is riskier because of the pathogenicity issue. It also requires maintenance of large cultures. Therefore, synthesis of nanocatalysts with greener methods is preferred because a cost-effective, simpler, and eco-friendly [4].

Nano Fe_3O_4 which is ferrimagnetic has wide application opportunities. The application of Fe_3O_4 in nanoparticle size is an alternative that is needed to meet the needs of industrial raw materials which are in development and their needs are increasing. Nanomagnetic particles have varied physical and chemical properties and can be applied in various fields [5]. These nanoparticles can be used as materials for drug delivery systems (Drug Delivery System = DDS), catalysts, Magnetic Resonance Imaging (MRI), and cancer therapy [6] [7]. In order to be applied in these various fields, it is very important to consider the particle size, magnetic properties, and surface properties of the nanoparticles themselves [5][8].

Surface functionalization of the particles and proper selection of solvents are important factors to prevent aggregation between particles and produce a thermodynamically stable colloidal solution. The surface of Fe_3O_4 can be stabilized by aqueous dispersion through the adsorption of citric acid. This happens because citric acid forms a coordination in the presence of a carboxylate. Carboxylates have an important influence on the growth of Fe_3O_4 nanoparticles and their magnetic properties. Increasing the concentration of citric acid causes a significant decrease in the crystallinity of Fe_3O_4 formation. In addition, the presence of citrate causes changes in the surface geometry. Its stability is highly dependent on the pH and concentration of the acid being adsorbed [9]. Fe_3O_4 coated with citric acid is shown in Figure 1.

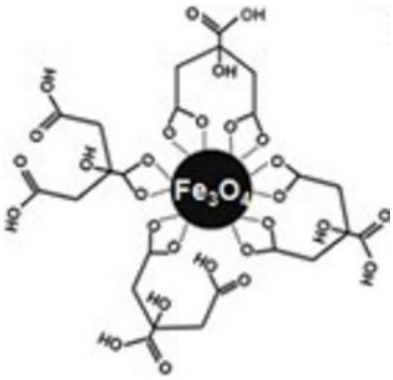

Figure 1. Fe_3O_4 *capped* Citric Acid

Brown seaweed with Sargassum filipendula species shown in Figure 2 is a potential source of bioactive compounds that are very useful for the development of the pharmaceutical industry such as antibacterial, antitumor, anticancer or as a reversal agent and the agrochemical industry, especially for antifeedants, fungicides and herbicides [10]. Alginate is a constituent of cell walls in seaweed which is commonly found in brown seaweed [11]. This compound is a heteropolysaccharide from the formation of monomer chains of mannuronic acid and gulunoric acid. Alginate content in seaweed depends on the type. The highest content of alginate (30-40% dry weight) can be obtained from Laminariales species while Sargassum only contains 16-18% dry weight [12].

Figure 2. Seaweed *Sargassum filipendula*

In a previous study, the synthesis of Fe_3O_4 nanoparticles was successfully carried out through bioreduction of $FeCl_3$ using the crude extract from brown seaweed Sargassum muticum which was characterized by a colour change from light yellow to blackish brown. It was assumed that the role in this reduction process is the sulfated polysaccharides found in seaweed. Sulfated polysaccharides contain hydroxyl, aldehyde, and sulfate functional groups [13][14]. This is evidenced from the FT-IR results where the sulfate group appears at wave number 1233 cm^{-1}, aldehyde at 1610 cm^{-1}, and a hydroxyl group at 3348 cm^{-1}. It begins with the involvement of the hydroxyl group in the hydrolysis of $FeCl_3$ to form $Fe(OH)_3$. Then in the presence of aldehydes, $Fe(OH)_3$ is reduced to form Fe_3O_4 while at the same time the aldehyde is oxidized to form the corresponding acid [15]. In this study, it will be observed how the role of Sargassum filipendula in the synthesis of nanocatalyst Fe_3O_4 capped citric acid (Fe_3O_4-CA).

Experimental

Preparation of Sulfated Polysaccharide Extract from Sargassum filipendula

The sample of Sargassum filipendula was taken from Binuangeun, Banten, Indonesia. Starting with the drying process using indirect sunlight for 10 hours, then aerated again at room temperature for 24 hours so that the water content is reduced making it easier to grind. Sargassum filipendula was crushed to obtain a dark brown powder. The powder was put into an Erlenmeyer then added with distilled water with a concentration of 5% by weight and boiled for 2 hours at a temperature of 100 °C. The suspension formed is filtered. The filtrate was added with 96% ethanol in a ratio of 1: 3 [15].

Preparation of Fe_3O_4 Nanoparticles

A total of 1 mmol $FeCl_3$ and 0.25 mmol $FeCl_2$ were added to 5 mL of Sargassum filipendula extract and 50 mL of distilled water as a medium for making nanoparticles. The mixture is stirred until homogeneous. Then 6 M NaOH was added little by little until it reached pH 10. The mixture was stirred for 2 hours and put in the oven [2].

Synthesis of Fe_3O_4-CA Nanocatalyst

A total of 2 grams of Fe_3O_4 was added with 250 mL of 1% citric acid. Heated to 60 °C and stirred for 60 minutes. The mixture was cooled at room temperature. The product was washed with distilled water and dried at 60 °C. The formed Fe_3O_4-CA nanocatalyst was characterized by PSA, SEM-EDX, and XRD [16].

Synthesis of Pyrimidine-derivative Compound

1 mmol of cinnamaldehyde was reacted with 2 mmol barbituric acid and 10% mol Fe_3O_4-CA with solvent-free. The catalysts are separated magnetically. The various of reaction time, amount of catalysts, solvent, and temperature are used for the optimization

Results and Discussion

The involvement of Sargassum filipendula in the synthesis of Fe_3O_4 nanoparticles is caused this seaweed contains various types of polysaccharides that can be used as metal reducing agents. Sargassum filipendula extract was taken by boiling seaweed (5% by weight) at 100 °C with distilled water for 1 hour, then filtered. The use of distilled water as a solvent is due to all the polysaccharides dissolved in it. The filtrate obtained was then added with ethanol (1:3 v/v), because ethanol can attract sulfated polysaccharides [15].

Figure 3 is a sulfated polysaccharide extract after being baked, in the form of a solid with blackish-brown colour. The presence of sulfated polysaccharides contained in this solid was confirmed by the appearance of elements C, O, and S in the analysis using EDX as shown in Table 1. While other elements such as Na, Mg, Al, and so on are minerals that are commonly contained in the seaweed. Sulfated polysaccharides contain sulfate, hydroxyl, and aldehyde groups which cause Fe^{3+} reduced and nanoparticle stabilized. Figure 4 is the FT-IR result of Sargassum filipendula extract showing the stretching vibration of C-O-SO_3 at 1040 cm^{-1}, at 1241 cm^{-1} indicating the presence of a sulfate group, aromatic C-C appearing at 1413 cm^{-1}. The wavenumber at 1604 cm^{-1} indicates the presence of carbonyl, 2932 cm^{-1} indicates the presence of C-H stretching vibrations, and at 3316 cm^{-1} indicates the presence of a hydroxyl group.

Figure 3. Sulfated polysaccharides

It begins with the involvement of a hydroxy group in the hydrolysis of $FeCl_3$ to form Fe $(OH)_3$ and release H^+ ions. $Fe(OH)_3$ is further reduced in the presence of seaweed extract to form Fe_3O4, while at the same time the aldehyde group in the sulfated polysaccharide is oxidized to form the corresponding acid. Fe_3O_4 nanoparticles that have been formed are then capped using citric acid. The surface of Fe_3O_4 can be stabilized by aqueous dispersion through the adsorption of citric acid. This happens because citric acid forms a coordination in the presence of a carboxylate. Carboxylates have an important influence on the growth of Fe_3O_4 nanoparticles and their magnetic properties. The magnetic properties of Fe_3O_4 and Fe_3O_4-CA are shown in Figure 5.

The purpose of Fe_3O_4 capping using citric acid (Fe_3O_4-CA) in addition to preventing agglomeration between particles, can also catalyze substrates in the synthesis of organic compounds through the carboxylic groups on the surface of Fe_3O_4 [1]. Fe_3O_4-CA was made using a simple method by adding 1% citric acid to Fe_3O_4 and stirring at 60 °C. The formation schema of Fe_3O_4-CA is shown in Figure 6, where MNP is a magnetic Fe_3O_4 nanoparticle and MNP-CA is Fe_3O_4 which has been capped with citric acid.

Table 1. EDX Results of *Sargassum filipendula*

Element	Composition (% Mass)
C	33.03 ± 1.70
O	47.03 ± 0.83
Na	2.20 ± 0.14
Mg	2.14 ± 0.28
Al	0.97 ± 0.23
Si	1.75 ± 0.42
S	2.26 ± 0.20
Cl	0.73 ± 0.20
K	5.59 ± 0.74
Ca	3.76 ± 0.22
Zn	0.54 ± 0.54

The crystal size was determined using the Debye-Scherrer equation with the formula $D = k.\lambda / \beta \cos \theta$. Where k is the crystal factor, λ is the wavelength used, β is the FWHM value in radians (1 radian = 57.3°), and θ is the Bragg diffraction angle. Table 2 shows that the β value of Fe_3O_4 in radian is 1.745×10^{-2}, the value of θ is 17.83, so that the D value is 8.34 nm. Table 3 shows that the β value of Fe_3O_4-CA in radian is 1.710×10^{-2}. The value of θ is 17.52. So that the D value of 8.5 nm is obtained. Crystal size obtained in this study smaller than without the use of Sargassum filipendula as previously reported with a crystal size of 10 nm [17].

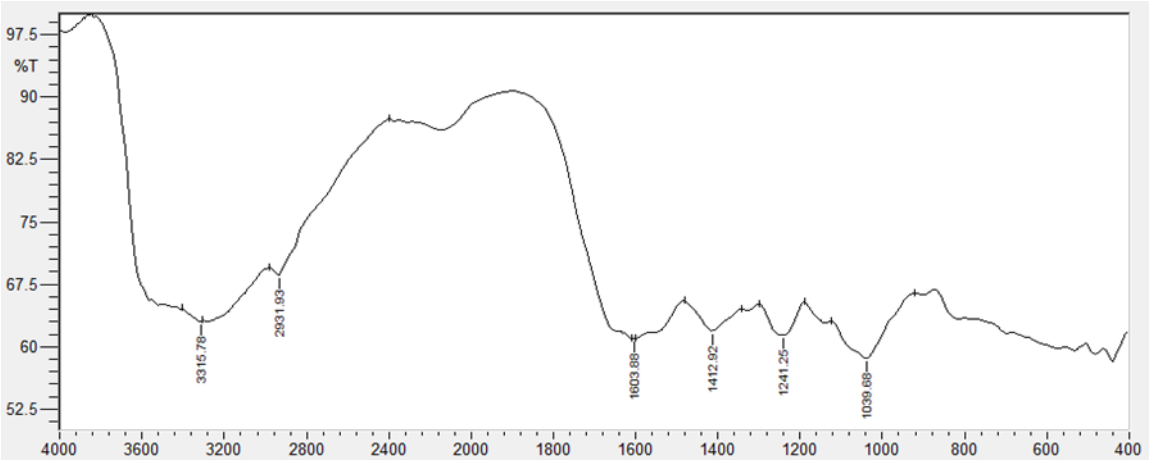

Figure 4. FT-IR Spectra of *Sargassum filipendula*

Particle size was characterized using the Particle Size Analyzer (PSA). The appropriate liquid medium used as a dispersion is 99% ethanol. Measurements were carried out seven times. The study results have obtained that the average particle radius is 30.41 nm for Fe_3O_4 and 45.09 nm for Fe_3O_4-CA. The graph of the relationship between the particle radius and intensity shown in Figure 7 and Figure 8.

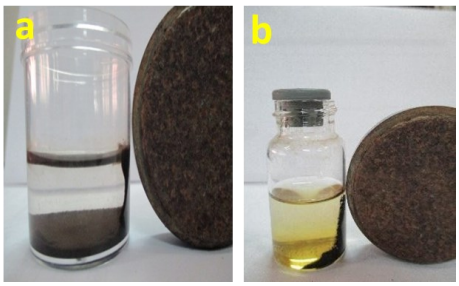

Figure 5. Magnetic Properties (a) Fe_3O_4, (b) Fe_3O_4-CA

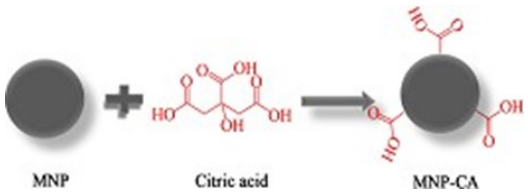

Figure 6. Proposed Reaction Mechanism for the Formation of Fe_3O_4-CA

Table 2. XRD Data of Fe_3O_4

 # Strongest 3 peaks

No.	Peak no.	2Theta (deg)	D (A)	I/I1	FWHM (deg)	Intensity (Counts)	Integrated Int (Counts
1	20	35.6600	2.51573	100	1.0000	56	3242
2	15	30.3200	2.94552	52	0.8000	29	1234
3	46	62.5800	1.48314	52	0.3000	29	444

Table 3. XRD Data of Fe_3O_4-CA

 # Strongest 3 peaks

No.	Peak no.	2Theta (deg)	d (A)	I/I1	FWHM (deg)	Intensity (Counts)	Integrated Int (Counts
1	25	35.0400	2.55881	100	0.0000	44	0
2	26	35.8200	2.50486	98	0.9800	43	2442
3	23	33.1700	2.69866	86	0.8200	38	2008

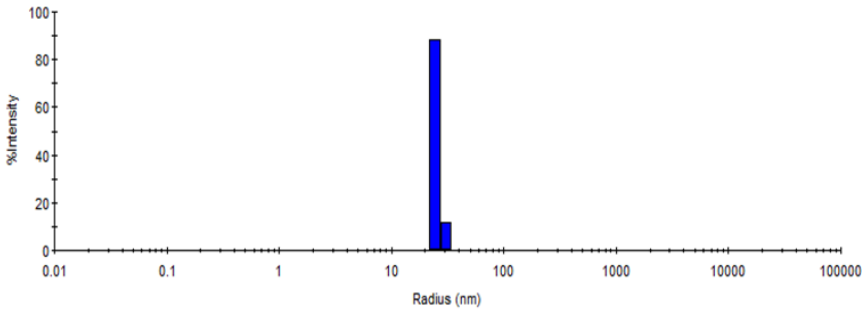

Figure 7. PSA Result of Fe_3O_4

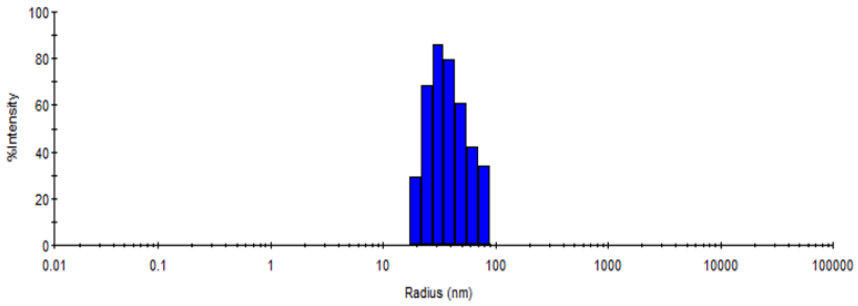

Figure 8. PSA Result of Fe_3O_4-CA

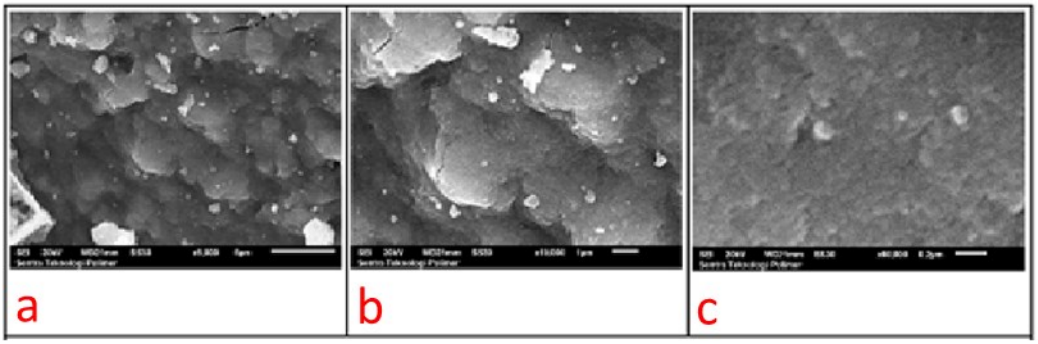

Figure 9. SEM result of Fe_3O_4 at (a) 5000x magnification (b) 10000x magnification (c) 60000x magnification

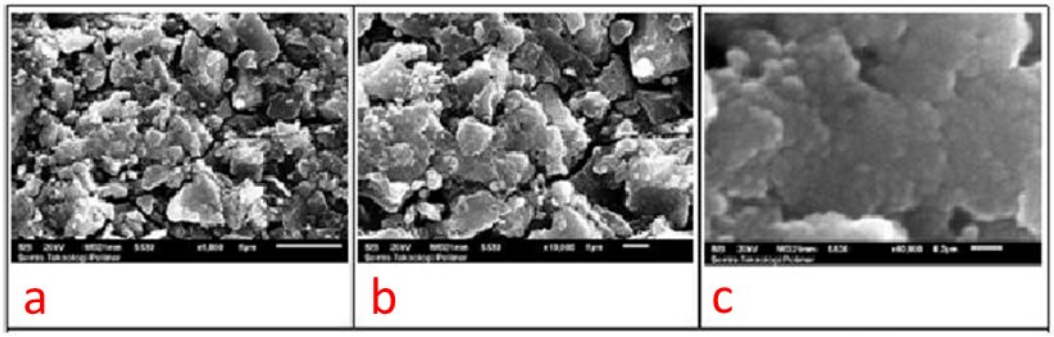

Figure 10. SEM result of Fe_3O_4-CA at (a) 5000x magnification (b) 10000x magnification (c) 60000x magnification

The SEM results in Figure 9 shows the morphology of Fe_3O_4 is granular and Fe_3O_4-CA in the form of granular and fiber. The morphological differences indicate that in Fe_3O_4-CA, the citric acid has capped Fe_3O_4 although in Figure 10 there's still a defect caused the uneven size of particles and the distribution is not homogenous. SEM-EDX presents qualitative and quantitative information of material components as in Table 4.

Table 4. EDX Result of Fe_3O_4 and Fe_3O_4-CA

Elements	Composition(% Mass)	
	Fe_3O_4	Fe3O4-CA
C	7.60 ± 3.11	15.17 ± 9.10
O	22.67 ± 11.58	36.11 ± 5.87
Fe	68.50 ± 15.67	48.72 ± 3.39

Characterized Fe_3O_4-CA nanocatalyst was tested on the synthesis of pyrimidine-derivative compound with optimum conditions at 7.5% mol catalyst and temperature of 50 °C for 6 hours with 83.2% yield obtained. Figure 11 shows this compound is yellow powder and plausible reaction mechanism with Fe_3O_4-CA nanocatalyst is in Figure 12.

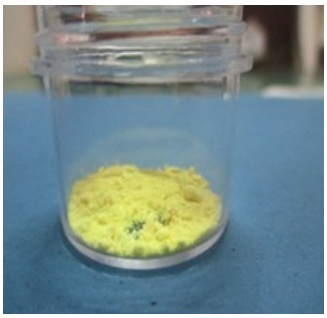

Figure 11. Pyrimidine-derivative Compound

Conclusion

Fe_3O_4-CA nanocatalyst from Sargassum filipendula polysaccharide extract had a crystal size of 8.5 nm and an average particle radius of 45.09 nm. This nanocatalyst was also tested on the synthesis of pyrimidine derivative compounds and obtained a yield of 83.2%. Fe_3O_4-CA nanocatalyst is heterogeneous catalyst that can remove easily after reaction using magnetic bar.

References

[1] H. Naeimi and Z. S. Nazifi, "A highly efficient nano-Fe_3O_4 encapsulated-silica particles

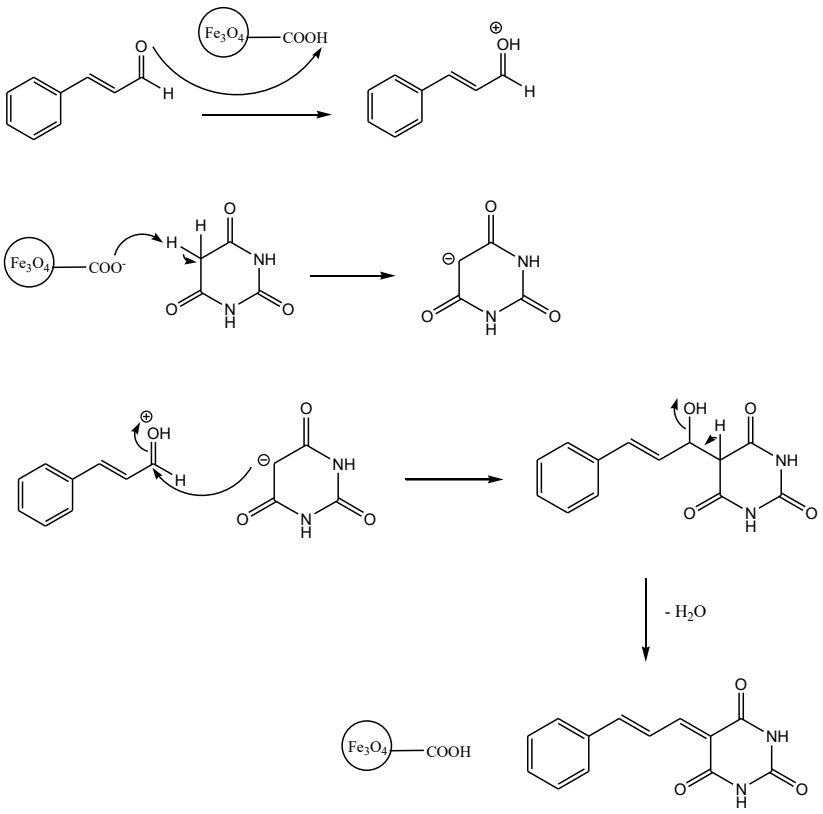

Figure 12. Plausible Mechanism of Pyrimidine-derivative Compound

bearing sulfonic acid groups as a solid acid catalyst for synthesis of 1,8-dioxo-octahydroxanthene derivatives," J. Nanoparticle Res., vol. 15, no. 11, 2013, doi: 10.1007/s11051-013-2026-2.

[2] Y. Xing et al., "Controllable synthesis and characterization of Fe3O4/Au composite nanoparticles," J. Magn. Magn. Mater., vol. 380, pp. 150–156, Apr. 2015, doi: 10.1016/j.jmmm.2014.09.060.

[3] F. G. Golmohamadi, F. Khodarahmi, S. P. Arbab, A. Moshaii, and E. Saievar-Iranizad, "Synthesis and properties of Fe_3O_4/CdTe Nanocomposite," Applied Surface Science, 301:244-249, 2012.

[4] G. Pal, P. Rai, and A. Pandey, "Green synthesis of nanoparticles: A greener approach for a cleaner future," in Green Synthesis, Characterization and Applications of Nanoparticle, 1-26, 2019, DOI: 10.1016/B978-0-08-102579-6.00001-0

[5] M. Kamalzare, M. R. Ahghari, M. Bayat, and A. Maleki, "Fe_3O_4@chitosan-tannic acid bionanocomposite as a novel nanocatalyst for the synthesis of pyranopyrazoles," Sci. Rep., vol. 11, no. 1, Dec. 2021, doi: 10.1038/s41598-021-99121-2.

[6] T. Vangijzegem, D. Stanicki, and S. Laurent, "Magnetic iron oxide nanoparticles for drug delivery: applications and characteristics," Expert Opin. Drug Deliv., vol. 16, no. 1, Jan. 2019, doi: 10.1080/17425247.2019.1554647.

[7] H. Amrulloh, A. Fatiqin, W. Simanjuntak, H. Afriyani, and A. Annissa, "Antioxidant and Antibacterial Activities of Magnesium Oxide Nanoparticles Prepared using Aqueous Extract of Moringa Oleifera Bark as Green Agents," J. Multidiscip. Appl. Nat. Sci., vol. 1, no. 1, Jan. 2021, doi: 10.47352/jmans.v1i1.9.

[8] A. Fadaka, O. Aluko, S. Awawu, and K. Theledi, "Green Synthesis of Gold Nanoparticles using Pimenta dioica Leaves Aqueous Extract and Their Application as Photocatalyst, Antioxidant, and Antibacterial Agents," J. Multidiscip. Appl. Nat. Sci., vol. 1, no. 2, May 2021, doi: 10.47352/jmans.v1i2.81.

[9] S. Sundar, S. J. Kwon, and G. Venkatachalam, "Magneto-Biosensor for the Detection of Uric Acid Using Citric Acid-Capped Iron Oxide Nanoparticles.," J. Nanosci. Nano-

technol., vol. 20, no. 4, 2020, doi: 10.1166/jnn.2020.17313.

[10] C. M. Coelho, J. R. de Andrade, M. G. C. da Silva, and M. G. A. Vieira, "Removal of propranolol hydrochloride by batch biosorption using remaining biomass of alginate extraction from Sargassum filipendula algae," Environ. Sci. Pollut. Res., vol. 27, no. 14, May 2020, doi: 10.1007/s11356-020-08109-4.

[11] C. M. P. G. Dore et al., "A sulfated polysaccharide, fucans, isolated from brown algae Sargassum vulgare with anticoagulant, antithrombotic, antioxidant and anti-inflammatory effects," Carbohydr. Polym., vol. 91, no. 1, pp. 467–475, Jan. 2013, doi: 10.1016/j.carbpol.2012.07.075.

[12] D. Rodrigues et al., "Chemical composition of red, brown and green macroalgae from Buarcos bay in Central West Coast of Portugal," Food Chem., vol. 183, pp. 197–207, Oct. 2015, doi: 10.1016/j.foodchem.2015.03.057.

[13] G. J. Wu, S. M. Shiu, M. C. Hsieh, and G. J. Tsai, "Anti-inflammatory activity of a sulfated polysaccharide from the brown alga Sargassum cristaefolium," Food Hydrocoll., vol. 53, pp. 16–23, Feb. 2016, doi: 10.1016/j.foodhyd.2015.01.019.

[14] P. Vijayabaskar and N. Vaseela, "In vitro antioxidant properties of sulfated polysaccharide from brown marine algae Sargassum tenerrimum," Asian Pacific J. Trop. Dis., vol. 2, no. SUPPL2, 2012, doi: 10.1016/S2222-1808(12)60287-4.

[15] M. Mahdavi, F. Namvar, M. Bin Ahmad, and R. Mohamad, "Green biosynthesis and characterization of magnetic iron oxide (Fe_3O_4) nanoparticles using seaweed (Sargassum muticum) aqueous extract," Molecules, vol. 18, no. 5, pp. 5954–5964, May 2013, doi: 10.3390/molecules18055954.

[16] H. Wang, X. Y. Qin, Z. Y. Li, Z. Z. Zheng, and T. Y. Fan, "Preparation and characterization of citric acid-modified superparamagnetic iron oxide nanoparticles," Beijing Da Xue Xue Bao., vol. 50, no. 2, pp. 340-346, 2018, online available: https://pubmed.ncbi.nlm.nih.gov

[17] E. Cheraghipour, S. Javadpour, and A. R. Mehdizadeh, "Citrate capped superparamagnetic iron oxide nanoparticles used for hyperthermia therapy," J. Biomed. Sci. Eng., vol. 05, no. 12, pp. 715–719, 2012, doi: 10.4236/jbise.2012.512089.